Analysis of temperature and humidity in Oman using Singular Spectrum Analysis

S. AL Marhoobi[a,b] and A. Pepelyshev[b*]

[a]Ministry of Higher Education, Research and Innovation, Oman; *[b]School of Mathematics, Cardiff University, Senghennydd Road, Cardiff, CF24 4AG, UK*

(*.... 2020*)

The purpose of this paper is to study hourly time series of temperature and humidity from six meteorological stations in Oman from 2009 to 2018. Since our data contains missing values due to device failures, we have compared several methods of imputation and found that regression with lagging is most reasonable. To extract the annual oscillations and daily periodicities from hourly time series we apply Singular Spectrum Analysis. By applying the Mann-Kendall test, Spearman's rho test and the ITM test to the annual oscillations and daily periodicities monotonic trends in temperature and humidity over the ten year period have not been confirmed.

Keywords: Singular Spectrum Analysis; imputation of missing values; Mann-Kendall test; ITM test

AMS Subject Classification: 62M20

1. Introduction

Finding changes in climate characteristics is attracting many researchers but not much is known about climate change in Oman. The authors of [1] provide a good picture about the past climate in Oman since 1961 and simulate future climate projections that have harmful consequences such as the increase of the minimum temperature and the decrease of rainfall. In [2], the authors found trends in temperature and rainfall records at the Saiq meteorological station in Oman over the period 1979–2012. In [3], the climate trends in mountain oases of northern Oman over the last three decades are reported. Oman is a country with an arid and semi-arid climate, where nature and agriculture is very sensitive to climate changes and water is an important limiting resource [1, 4, 5]. Meteorological trends serve as indicators of climate change and should be used by policy makers to maintain the ecosystem in the wealthy state.

In the present paper we investigate the hourly temperature and humidity time series collected at six meteorological stations in Oman from 2009 to 2018. This data is provided by the Directorate General of Meteorology of Oman and has not previously been studied in the literature. Our investigation will be segmented into three parts: (i) missing value imputation, (ii) splitting the hourly time series in the sum of several components corresponding to different frequencies, and (iii) detection of trends.

Missing data in hourly meteorological time series usually occur due to device failures [3]. Since statistical procedures require time series without missing values, we investigate three methods for filling gaps in time series: the iterative approach using Singular

---

Spectrum Analysis (SSA) [6], the multiple regression method and regression with lagging.

From the hourly time series we extract components such as the annual and daily oscillations using SSA which is a non parametric, powerful method for time series analysis. In general, SSA can be used for parametric estimation, forecasting and gap filling amongst many other tasks [6–10]. SSA is very useful for extracting various signals from noisy observations [11]. SSA provides meaningful results in many research areas without making any restrictive assumptions on the processed data. In [6], SSA was used for the extraction of seasonality, simultaneous extraction of cycles with small and large periods and finding structure in short time series. The core of SSA relies on decomposing the original time series data into a sum of a small number of components with use of the singular value decomposition of a trajectory matrix, see [6]. In many applications, the components extracted by SSA can be identified as trends, periodic components or noise. Many scientific papers in the last two decades have used SSA as an effective tool for analysing and forecasting time series.

To detect trends in temperature and humidity we apply the Mann-Kendall test, Spearman's rho test and the ITM test [12]. The latter test is less restrictive than the others and is already widely applied to various meteorological time series. For example, the ITM test showed trends in monthly streamflows in northern regions of Turkey during 1964–2007, see [13], trends in monthly rainfalls in a region of Ethiopia during 1980–2016, see [14], showed and trends in annual temperature in China during 1960–2015, see [15].

The present paper is organized as follows. Section 2 contains a description of the meteorological data of Oman. Section 3 provides a brief description of the methodology of SSA. Section 4 describes the three aforementioned methods for imputation. Section 5 contains a numerical study of the data imputation methods. Section 6 investigates annual oscillations of temperature and humidity. Section 7 contains results about daily periodicities for hourly time series. Finally, conclusions are given in Section 8.

2. Meteorological data of Oman

We consider hourly temperature (measured in Deg c), humidity (measured in %) and precipitation (measured in mm) collected at six meteorological stations in the Sultanate of Oman from 2009 to 2018. These stations are located in Khasab Airport (K), Masirah (MA), Muscat International airport (MU), Saiq (SQ), Salalah (SA) and Thumrait (TH) and are shown in Figure 1. The hourly meteorological data was provided to us by the Directorate General of Meteorology of Oman.

Let us briefly highlight the major climate and geographic specifics of Oman, see [1] for a more precise climatic description. Oman is located on the southeastern corner of the Arabian Peninsula in southwest Asia. The climate in Oman is hot and dry from May to the end of October and has mild winters, except for the south of country. Also, south of Oman is affected by a monsoon climate from June to September.

The individual specifics of six meteorological stations are as follows.

- Khasab (K) is located in Musandam Governorate which is a mountainous Omani peninsula and has wet summers and rainy, cold winters.
- Masirah Island (MA) is the largest island in Oman and has hot summers and warm winters.
- Muscat (MU) is a capital of Sultanate of Oman. The city lies on the Arabian Sea along the Gulf of Oman. It has very hot summers and warm winters.
- Saiq (SQ) is located in the mountain of Al Jabal Al Akhdar city. It is one of the highest points in Oman and eastern Arabia. Temperature drops during winter to below zero Celsius, with snow falling, and rises in the summer to typically 22 degrees Celsius.
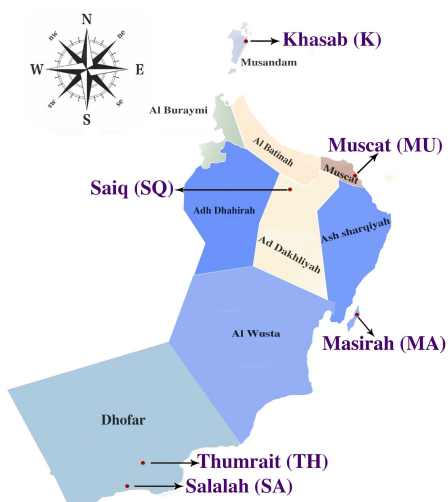
Figure 1. Map of Oman with locations of stations.

- Salalah (SA) is the capital and largest city of the southern Oman governorate of Dhofar. It is very cloudy and foggy from July to August with little rain fall.
- Thumrait (TH) is a town of the Dhofar Governorate in southern Oman. It has mild summers and warm winters. Rainfall occurs from February to April, as well as June to August due to the monsoon.
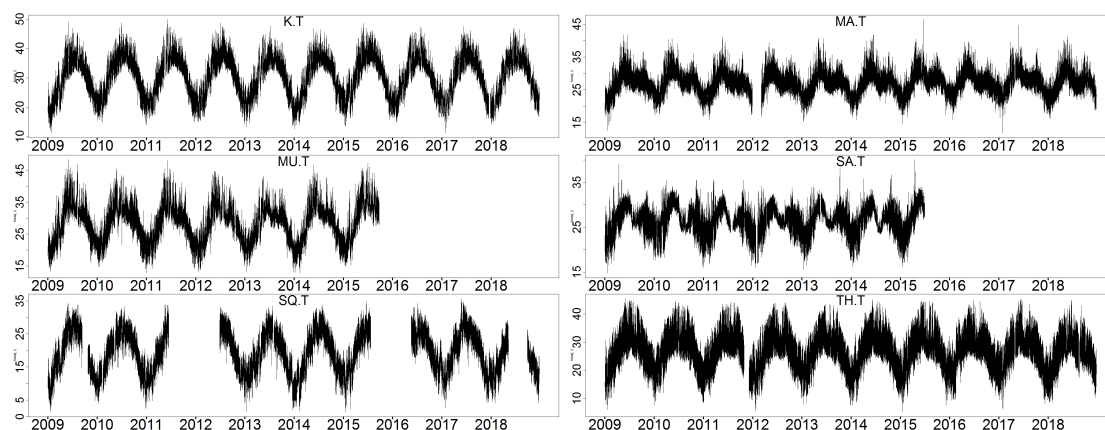

Figure 2. Hourly temperature at six meteorological stations.

We show hourly time series of temperature in Figure 2. We can see that the lowest temperature is observed at the station SQ and the highest temperature is recorded at the station K. The annual temperature pattern has a sinusoidal shape in stations K, MU, SQ and TH and a two-mode shape in stations MA and SA.

We depict hourly time series of humidity in Figure 3. We can observe that humidity is very volatile. The annual pattern is clearly visible for the station SA and slightly visible for stations MA and MU. The high humidity is more often observed at the station MA.

Precipitation in Oman occurs very rarely and, therefore, graphs of hourly time series of precipitation would not be appropriate. As a result, in Figure 4, we show the cumulative precipitation. We can see that precipitation usually occurs in winter months and the larger precipitation was observed in stations SQ and K, while the lower precipitation is recorded in stations TH and SA. The station TH is remarkable due to very long periods with no precipitation.
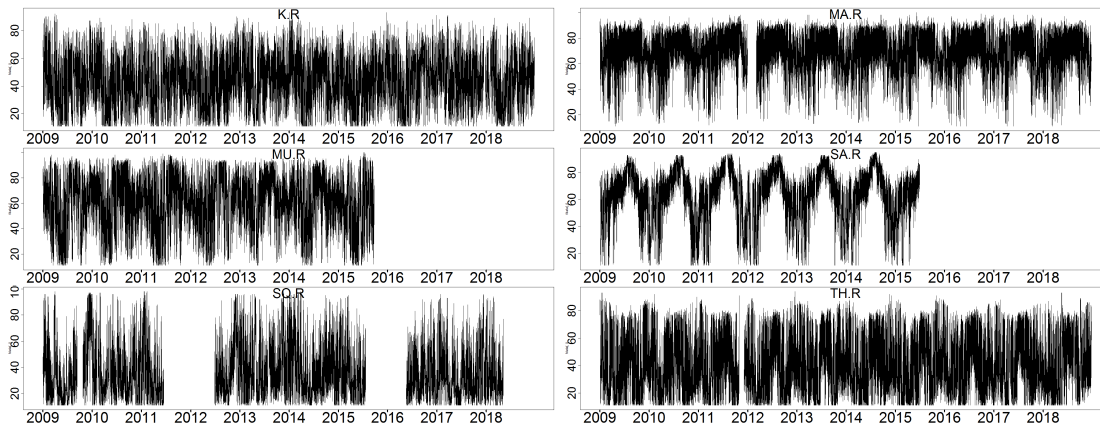
3

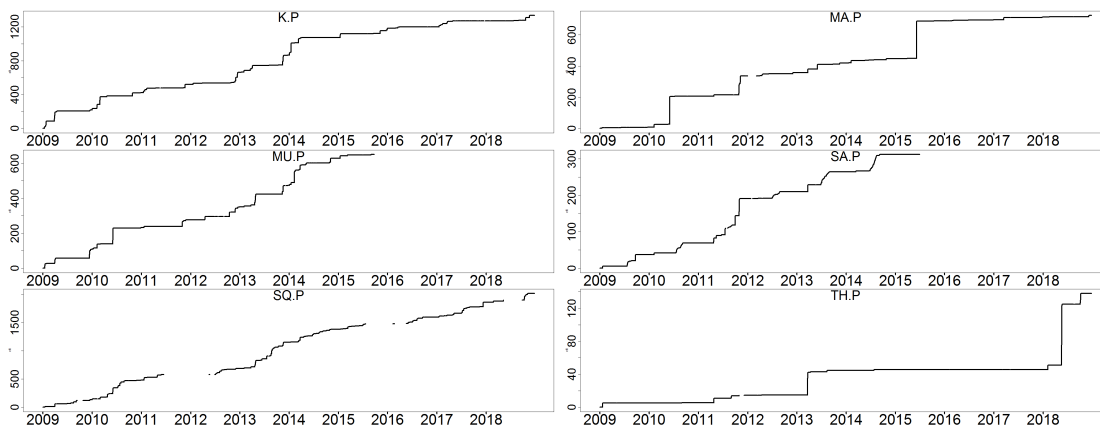Figure 3. Hourly humidity at six meteorological stations.

Figure 4. Cumulative precipitation at six meteorological stations.

3.   Basic SSA

Basic SSA is a core version of SSA and primarily consists of embedding a time series to the space of Hankel matrices and subsequent decomposition into rank-one matrices by use of the conventional singular value decomposition. By then inverting embedding procedure, SSA yields a decomposion of the original time series into the sum of a small number of components such as a slowly varying trend, oscillatory components and noise [6, 9]. Using traditional notation, SSA is performed in two stages:

- Decomposition stage: embedding and singular value decomposition.
- Reconstruction stage: grouping and diagonal averaging.

Basic SSA can strictly be described as follows. Let $x_1, x_2, \ldots, x_N$ be a time series. For a given window length L $(1 < L < N)$, we construct the L-lagged vectors $X_{(i)} = (x_i, \cdots, x_{i+L-1})^T$, $i = 1, 2, \ldots, K = N-L+1$, and compose these vectors into the matrix

$$\mathbf{X} = (x_{i+j-1})_{i,j=1}^{L,K} = \left[X_{(1)}, \ldots, X_{(K)} \right].$$

This matrix has size $L \times K$ and is often called 'trajectory matrix'. It is a Hankel matrix, which means that all the elements along the diagonal $i+j =$const are equal. The singular-value decomposition of the matrix $\mathbf{X}\mathbf{X}^T$ yields a collection of L eigenvalues and eigenvectors. For a given integer r when $1 < r < L$ we create a group using r largest eigenvalues and corresponding eigenvectors of $\mathbf{X}\mathbf{X}^T$. The chosen eigenvectors de-

termine an r-dimensional subspace in R^L which is denoted as S_r. The L-dimensional data $X_{(1)}, \ldots, X_{(K)}$ is then projected onto this r-dimensional subspace S_r and the subsequent averaging over the diagonals gives us some Hankel matrix $\tilde{\mathbf{X}}$, which we consider as an SSA approximation to $\mathbf{X}$. With a proper choice of r and L, the time series corresponding to $\tilde{\mathbf{X}}$ is often used as an estimator of a signal or a trend. The main guideline for selecting r and L is to take sufficiently large, say $L \approx \frac{N}{2}$ and, if we want to extract a periodic component with known period, to take the window length to be divisible by the period, while r is chosen on the base of relations between eigenvalues and the spectral properties of eigenvectors considered as time series, see [6].

4.   Missing data

Meteorological data in our study contain instrumental errors and missing values which are shown in Figures 2–4. To run traditional algorithms of time series analysis, we have to perform imputation. The simplest methods like mean, median and mode imputation are not reasonable because with have data in form of time series. In this section we study three methods of replacing missing values: (i) the SSA-based iterative approach, (ii) the regression method and (iii) regression with lagging.

The SSA-based iterative approach to imputation in time series was proposed in [16]. This approach consists of filling in missing values using some initial values and iteratively improving these values via the SSA approximations. At each iteration, the recently computed values from the SSA approximation are inserted to the places of missing entries. This approach works well when the missing entries are initially filled in using some reasonable values [6]. This approach is implemented in the function *igapfill* in the R package *Rssa* [17]. We applied this function with the window length $L = 120$ and the number of components r which minimizes the mean square error of retrospective forecasts [6, Sect. 3.5.7].

Multiple regression imputation is applied to data in the form of a matrix, where columns correspond to variables and rows correspond to observations. For a variable with missing values, we create several subsets of complete observations and build several regression models. These models give several predicted values and their pooling provides a value for imputation. In our study we used multiple regression imputation implemented in the SPSS program with a pooling of 5 predicted values.

4.1.   *Imputation by regression with lagging*

In this subsection we describe an imputation procedure using regression with lagging. Recall that our data is several time series observed at six locations of Oman and it is natural that these time series are correlated. Since distances between some locations is quite big, changes in meteorological characteristics may occur with some lag. Also, time series may have specific periodic patterns which are individual to the locations of meteorological stations. Thus, we consider the following model for a time series at the i-th location

$$y_i(t) = \beta_0 + \beta_i P(t - \lfloor t \rfloor) + \sum_{j \neq i}^{K} \beta_j y_j(t - L_j) + \varepsilon(t), \tag{1}$$

where $P(t)$ is the annual pattern calculated by taking the average across several years, $\lfloor t \rfloor$ stands for the integer part operation, and $\beta_0, \beta_1 \ldots, \beta_K, L_1, \ldots, L_K$ are parameters to be estimated.

We assume that the model (1) holds for short time intervals $[t_1, t_2]$ and parameters may depend on time. Since time series are correlated, there exists a problem of collinearity and therefore we will estimate parameters such that the parameters $\beta_1 \ldots, \beta_K$ are positive. To avoid the computational burden in the global estimation problem, we estimate parameters $L_1, \ldots, L_K$ independently. Specifically, we choose L_j to maximize the cross-correlation between $y_i(t)$ and $y_j(t)$.

In general, observations at time t for one variable are likely to be correlated with observations of other variables at times $(t-1)$, $(t-2)$ and so on. The model (1) includes variables with lagging just at time $(t-L)$ since the inclusion of more lagged variables at $(t-L-1)$ and $(t-L+1)$ shows minimal improvements in accuracy [18].

5. Numerical study of data imputation methods

In Figures 5–7 we show the segments of temperature time series with missing values imputed by the SSA-based iterative approach and by regression with lagging. The imputed values are shown in red and non-missing values are shown in black.
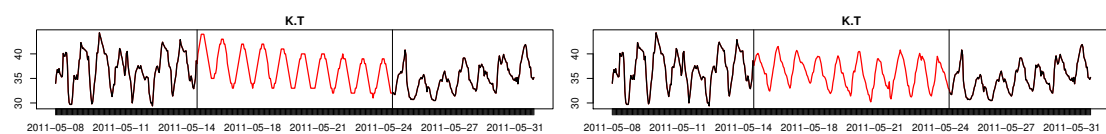

Figure 5. Temperature at the station K with non-missing (black) and imputed (red) values in May 2011. Left: The SSA-based iterative approach. Right: Imputation by regression with lagging.

We can see that the SSA-based iterative approach works well for imputing short gaps, up to a couple of days, see, e.g., Figure 6. If missing values create a long gap, then the imputed values look almost like a clear periodic wave with a linear trend. For example, in Figure 5 a periodic wave has the form of sinusoid which is an aggregation of neighbour daily cycles. In contrast, imputation by regression with lagging yields more realistic values.
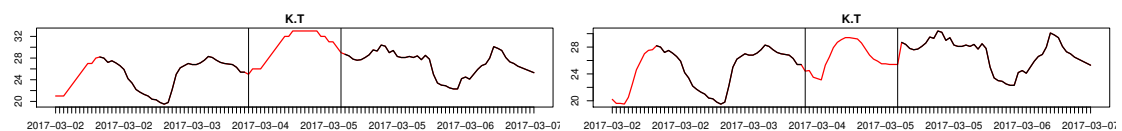

Figure 6. Temperature at the station K with non-missing (black) and imputed (red) values in March 2017. Left: The SSA-based iterative approach. Right: Imputation by regression with lagging.
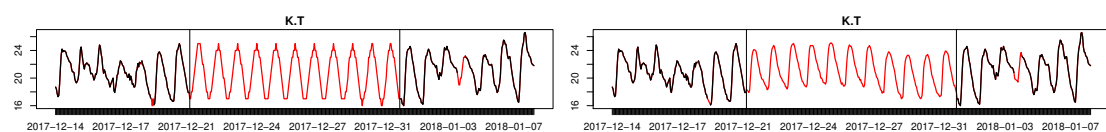

Figure 7. Temperature at the station K with non-missing (black) and imputed (red) values around New Year 2018. Left: The SSA-based iterative approach. Right: Imputation by regression with lagging.

In Figure 7, we observe that the missing values imputed by the SSA-based iterative approach do not contain the day-to-day variations in the temperature amplitude and, thus, this method cannot be recommended for filling in long gaps into time series with unstable structure.

In Figures 8–12, we compare multiple regression imputation (left panel) and imputation by regression with lagging (right panel) applied to humidity and temperature time series.
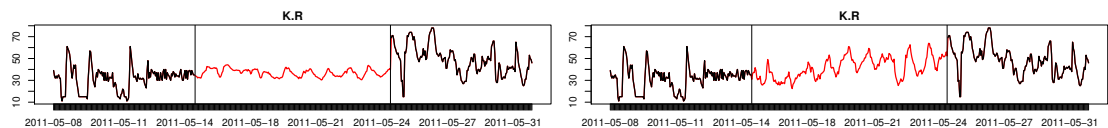
6

Figure 8. Humidity at the station K with non-missing (black) and imputed (red) values in May 2011. Left: Multiple regression imputation. Right: Imputation by regression with lagging.

In Figure 8, we see that humidity is almost constant during two days before a gap with missing values and has non-regular fluctuations after the gap. Multiple regression imputation fills the gap by daily oscillations of very small magnitude. Imputation by regression with lagging fills by a non-regular daily oscillation of small amplitude at the left part and large amplitude at the right part of the gap. Thus, imputation by regression with lagging looks more natural.
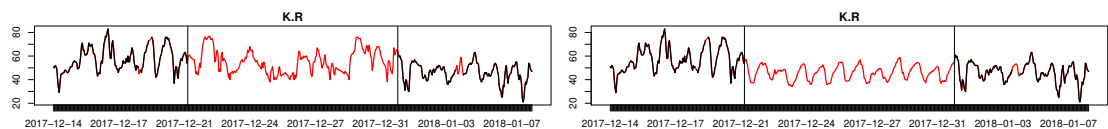

Figure 9. Humidity at the station K with non-missing (black) and imputed (red) values around New Year 2018. Left: Multiple regression imputation. Right: Imputation by regression with lagging.

In Figure 9, we observe that humidity has non-regular oscillations around a gap with missing values. Multiple regression imputation fills by values with disturbed daily oscillations. But Imputation by regression with lagging produces imputed values with clear daily oscillations. The former method is more reliable.
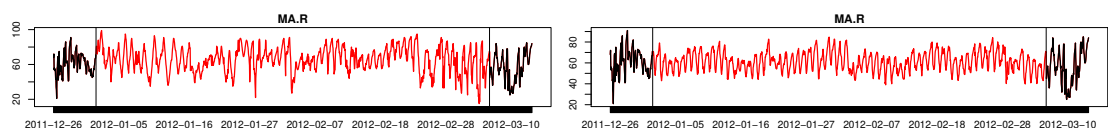

Figure 10. Humidity at the station MA with non-missing (black) and imputed (red) values around New Year 2012. Left: Multiple regression imputation. Right: Imputation by regression with lagging.

In Figure 10, we depict humidity time series with a big gap of missing values. Here both multiple regression imputation and imputation by regression with lagging produce reasonable results.
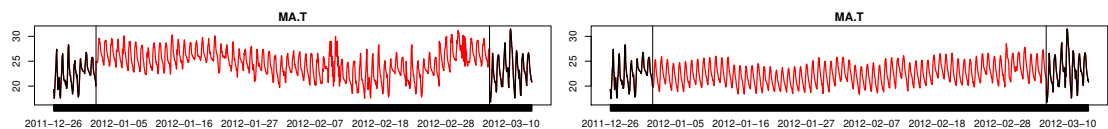

Figure 11. Temperature at the station MA with non-missing (black) and imputed (red) values around New Year 2012. Left: Multiple regression imputation. Right: Imputation by regression with lagging.

In Figure 11, we depict temperature time series around the same big gap as in Figure 10. Multiple regression imputation produces daily oscillations with rather large trend. But imputation by regression with lagging gives imputed values with a reasonable trend.
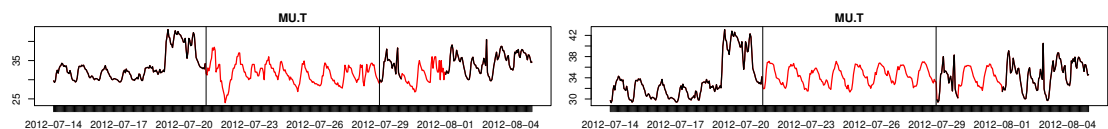

Figure 12. Temperature at the station MU with non-missing (black) and imputed (red) values around June 2012. Left: Multiple regression imputation. Right: Imputation by regression with lagging.

Figure 12 shows temperature time series at the station MU. Multiple regression imputation gives rather non-regular missing values. However, imputation by regression with lagging yields more sensible daily oscillations. For short gaps of missing values, both Multiple regression imputation and imputation by regression with lagging give similar results, which are not shown here due to lack of space.

Finally, in Figure 13 we compare imputation methods using temperature time series with artificial gaps. We can observe that imputation by regression with lagging is more accurate than imputation by the SSA-based iterative approach.
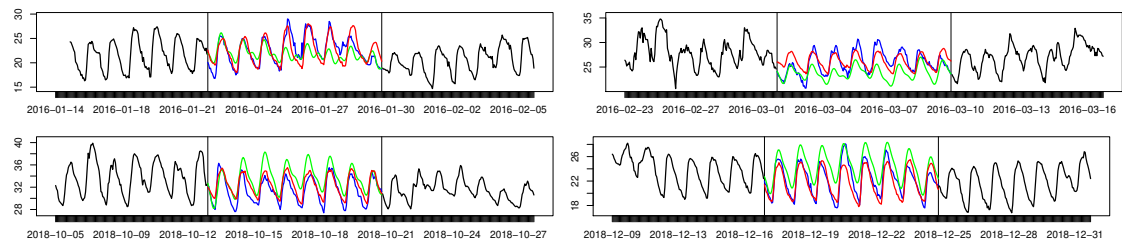

Figure 13.   Temperature at the station K with non-missing values (black curve). The blue curve corresponds to the observed values which are artificially missed. The green curve corresponds to values obtain by the SSA-based iterative approach. The red curve corresponds to values obtained by imputation by regression with lagging.

Our conclusion on comparison of three methods of imputation is that imputation by regression with lagging produces a more reliable imputation.

6.   Annual oscillations of temperature and humidity

The annual oscillations for hourly time series can be viewed as a trend (a slowly changing component) and, therefore, can be extracted as the first component of the SSA decomposition with a small window length [6]. We selected the window length $L = 5 \cdot 24 = 120$ that corresponds to the number of hours in 5 days.

In Figure 14 we depict hourly time series of the annual oscillations of temperature for six stations. We can see a small variation of temperature from year to year and random fluctuations from week to week. Also we see that the annual oscillation have a sinusoidal shape at stations K, MU and SQ and the two-saw shape in stations MA, SA and TH.
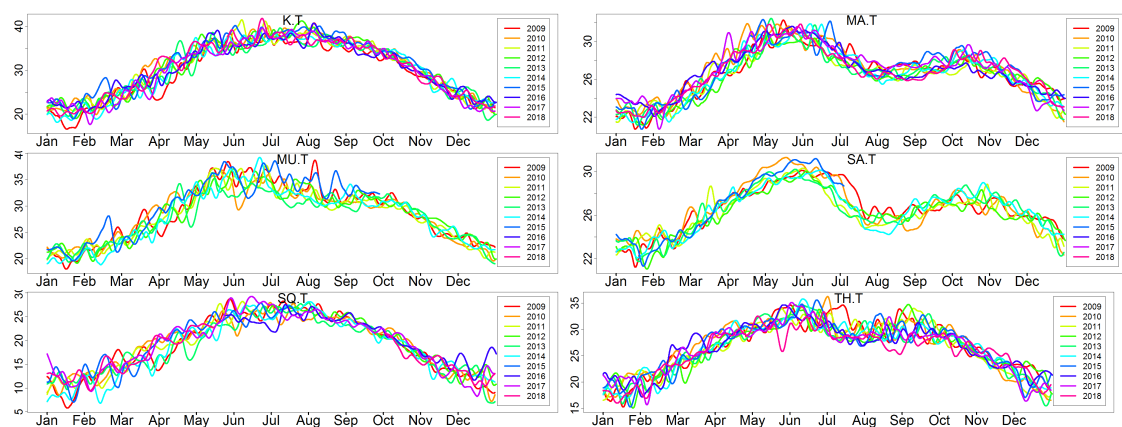

Figure 14. The annual oscillations of temperature at six stations.

In Figure 15 we depict the annual oscillations of humidity. We can see very large random variation of humidity from one week to another except summer months at stations MA

and SA. The lowest humidity is observed at the station SQ during almost all year and the highest humidity occurs in July–August at the station SA.
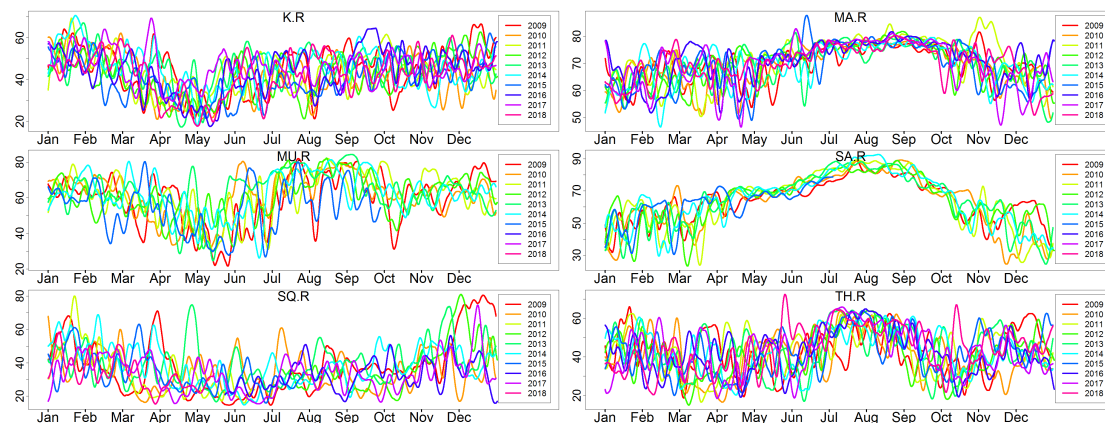

Figure 15. The annual oscillations of humidity at six stations.

To investigate for the presence of trends in the annual oscillations we will use the Mann-Kendall test, Spearman's rho test and the ITM test, see [5, 19, 20]. These tests are widely used to identify monotonous patterns in weather, climate or hydrology and to measure the importance of hydrometeorological time series patterns [13–15, 21, 22]. We apply three tests individually to sequences of length 10 generated for each hour of year across 10 years. The first two tests should be applied under assumptions of independence and normality which can be assumed to be satisfied for our data. Also, the power of the tests largely depends on the length of sequences which is rather short in our study.

The Mann-Kendall test is based on the statistic

$$S_{MK} = \sum_{i=1}^{N-1} \sum_{j=i+1}^{N} \text{sgn}(x_j - x_i),$$

where N is the length of a time series $x_1, \ldots, x_N$ and $\text{sgn}(\cdot)$ is the sign function. Spearman's rho test is based on the Pearson correlation coefficient between ranks and can be computed by

$$S_{SR} = 1 - \frac{6}{N(N^2 - 1)} \sum_{i=1}^{N} (R_i - i)^2,$$

where R_i is the rank of the i-th element of a time series. The ITM test is based on the statistic

$$S_{ITM} = \frac{2}{N} \Big(\text{mean}(x_{N/2+1}, \ldots, x_N) - \text{mean}(x_1, \ldots, x_{N/2}) \Big)$$

where $\text{mean}(\cdot)$ is the mean of a sequence. Using distributions of these tests, we compute the significance level for the hypothesis that the trend in data is absent.

Note that we perform multiple testing and, therefore, some p-values can be below 0.05 by chance. We found that the empirical distribution of 8760 p-values for each test is rather uniform for all three tests. Since the presence of a significant p-value for one particular hour is not important, we study the allocation of significant p-values along days in a year. Specifically, we show the cumulative number of significant p-values in Figures 16 and 17 for 6 stations. Since there are many missing values in Nov-Dec for locations MU

and SA, p-values for this period were not computed. These figures show several jumps meaning that there are few days in year with many significant p-values. Since the height of these jumps is not sufficiently large, we conclude that there is no monotonic trend in the annual oscillations of temperature and humidity over the period 2009-2018.
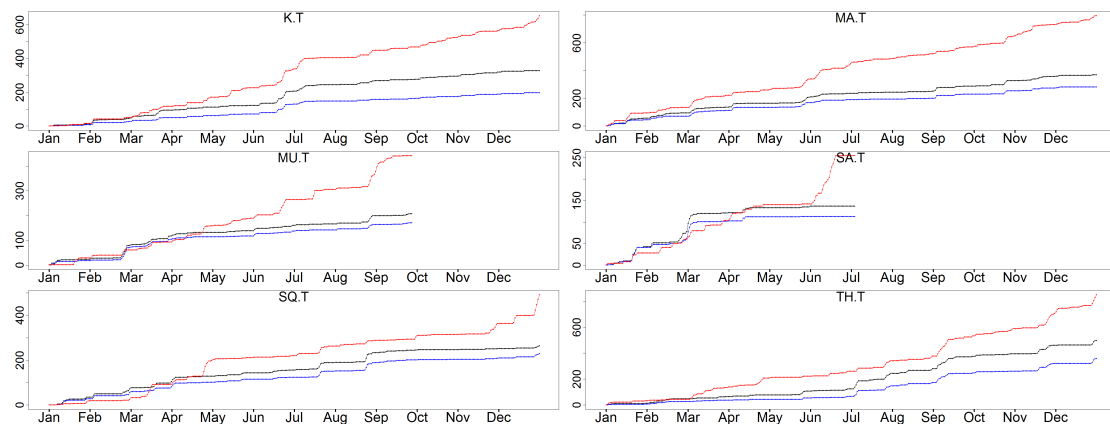

Figure 16.   The cumulative numbers of significant p-values of the Mann-Kendall test (black), Spearman's rho test (blue), the ITM test (red) for the annual oscillation of temperature in 6 locations.
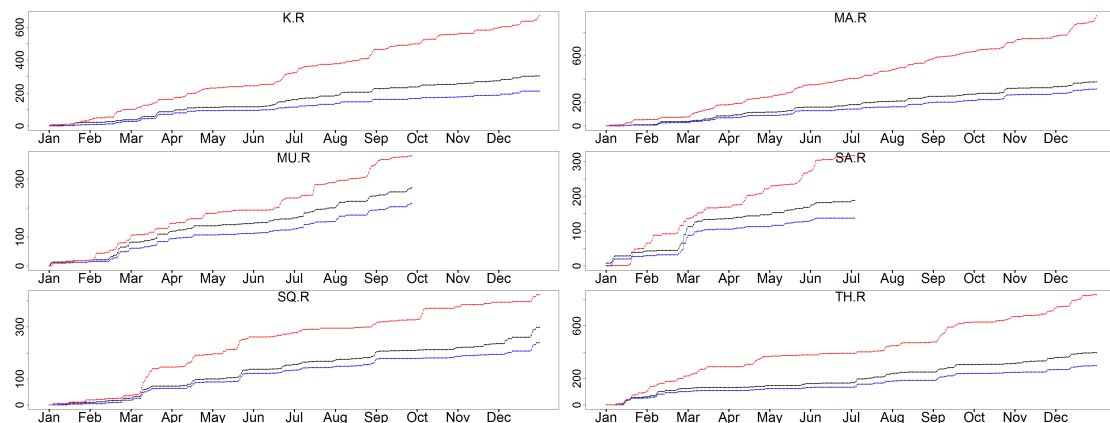

Figure 17.   The cumulative numbers of significant p-values of the Mann-Kendall test (black), Spearman's rho test (blue), the ITM test (red) for the annual oscillation of humidity in 6 locations.

For monthly temperature and humidity time series of length 120, we depict the ITM diagnostic in Figure 18 which compares the empirical distributions of the first and second halves of time series [20]. We can observe that the ITM diagnostic shows the absence of the trend in annual oscillations of monthly temperature and humidity at all stations.

7.   Daily periodicities

The daily periodicities for a hourly time series can be obtained by subtracting the leading component of the SSA decomposition with $L = 24$ from the analysed time series [6]. In Figure 19 we show the daily periodicities of temperature for six stations in July. We can see that the daily periodicities is very similar from year to year and from day to day within a month except the station MU. However, the shape of periodicities depends on stations. Also we applied the Mann-Kendall test, Spearman's rho test and the ITM test to values of the daily periodicities with one year increment and can conclude that there is no monotonic trend in the daily periodicities of temperature.
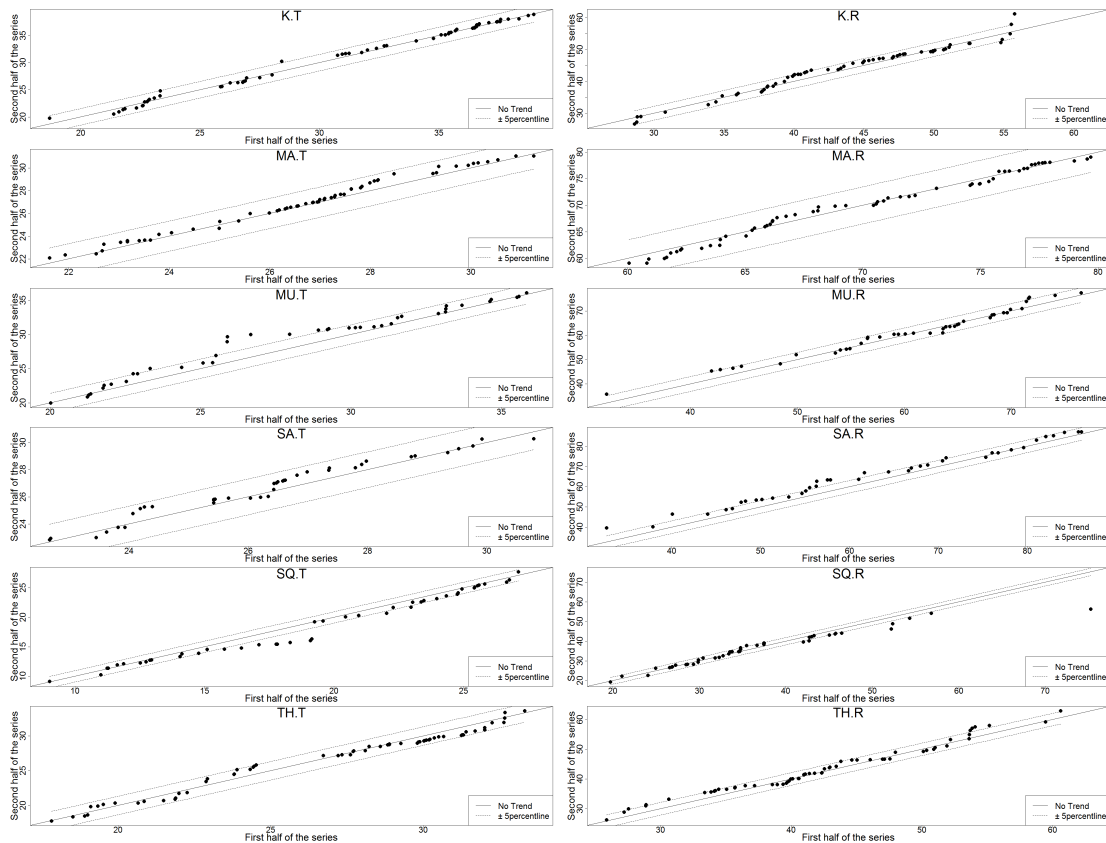
Figure 18. The ITM diagnostic of monthly time series of temperature (left) and humidity (right) in 6 locations.
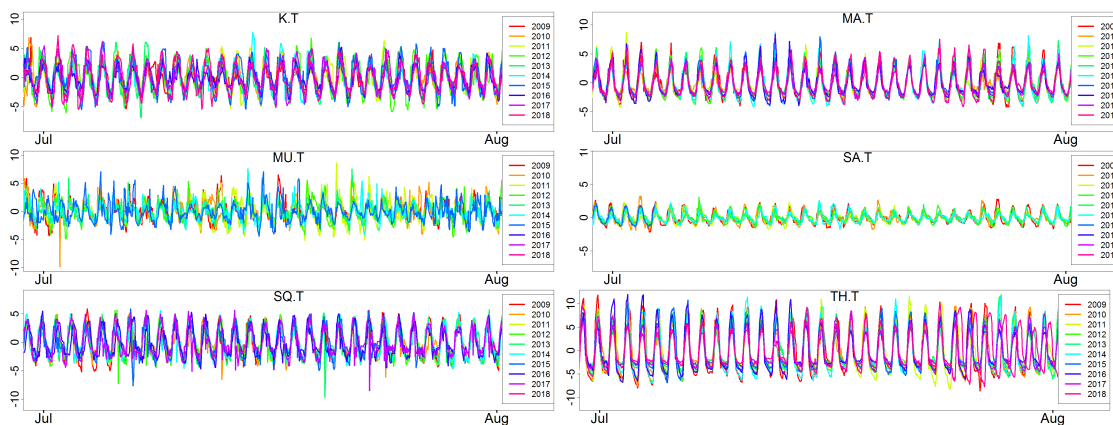

Figure 19. The daily periodicities of temperature in July at six stations.

In Figure 20 we depict the daily periodicities of humidity in July for six stations. We can see that the daily periodicities of humidity have a very small amplitude at the station SA, sharply replicates from year to year and from day to day within July at the stations MA and TH, and is very volatile at stations K, MU and SQ.

For studying the variability of the daily periodicities along year we consider the standard deviation of hourly time series of each month, specifically, we compute

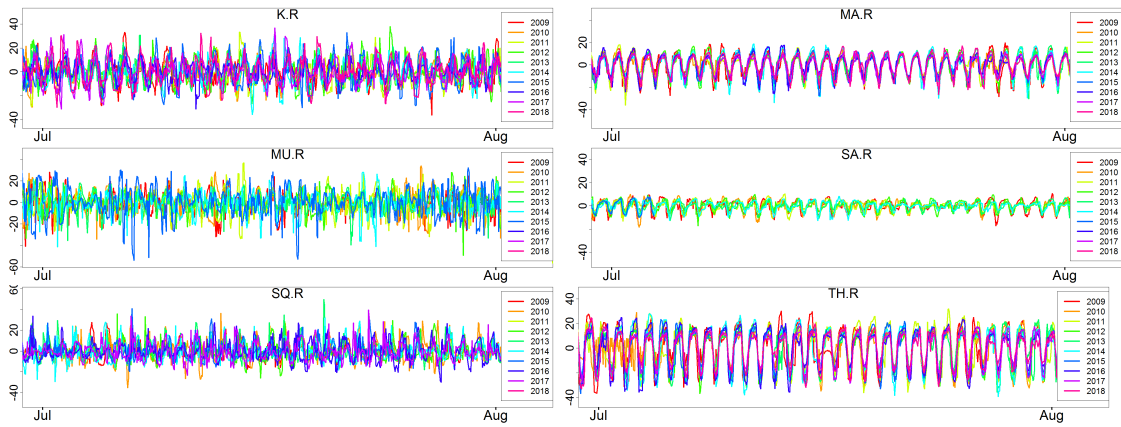$$s_m = \sqrt{\sum_{t=h_1(m)}^{h_2(m)} x_t^2}$$

11

Figure 20. The daily periodicities of humidity in July at six stations.

where $h_1(m)$ is the first hour of the m-th month, $h_2(m)$ is the last hour of the m-th month.
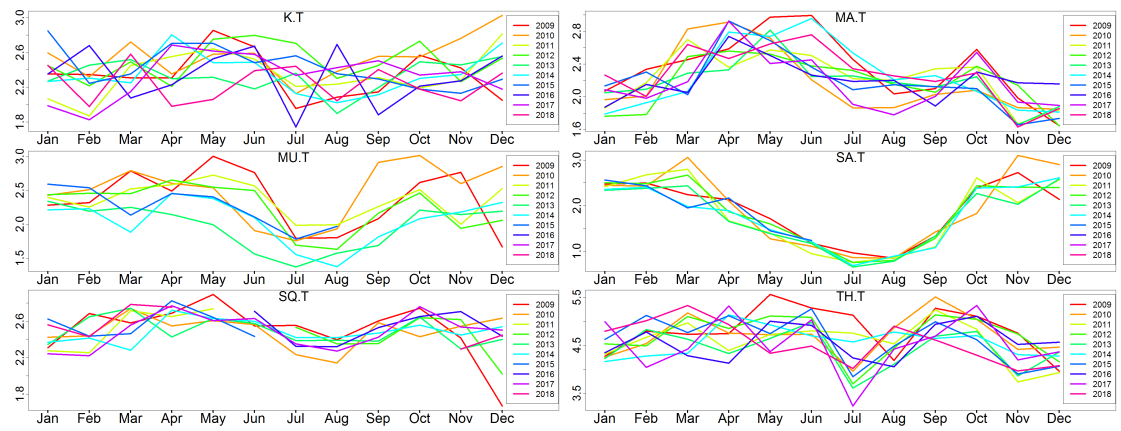

Figure 21. The monthly standard deviation of the daily periodicities of temperature.

In Figure 21 we can see that variability of the daily periodicities of temperature does not depend on the month at stations K, SQ and TH but it strongly depends on the month at stations MA, MU and SA. The Mann-Kendall test does not detect monotonous trends in monthly variability of the daily periodicities of temperature from year to year.
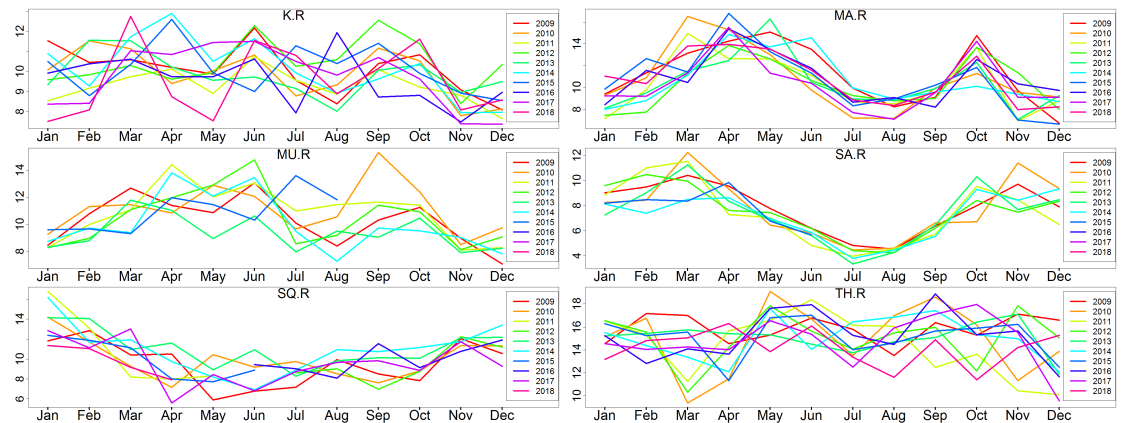

Figure 22. The monthly standard deviation of the daily periodicities of humidity.

In Figure 22 we can see that variability of the daily periodicities of the humidity is almost independent of the month for stations K and TH but it strongly depends on the month at stations MA and SA. Trends in monthly variability of the daily periodicities of humidity from year to year were not found by the Mann-Kendall test, Spearman's rho test and the ITM test.

8. Conclusion

In this paper we analyzed hourly time series of temperature and humidity from six meteorological stations in Oman from 2009 to 2018, which is to best of our knowledge the first paper studying such high frequency meteorological data from all parts of Oman. Firstly, we investigated three methods of imputation: SSA-based iterative approach, regression methods and regression with lagging. We found that imputation by regression with lagging is a more reliable and reasonable method and provides natural results for filling gaps for any length.

Secondly, we applied SSA to hourly time series for extracting the annual oscillations and the daily periodicities. SSA was able to extract these components very efficiently. Moreover, we may use SSA for obtaining more refined decompositions with larger number of components and also for forecasting.

Thirdly, we applied three commonly used tests for detecting trends in time series: the Mann-Kendall test, Spearman's rho test and the ITM test. We found that there are no monotonic trends in the annual oscillations and the daily periodicities over the period of ten years. Also we did not find trends in the monthly variability of daily periodicities.

The developments of this paper have been started to respond an enquiry from Research Council of Oman and will contribute to the national capacities of Oman in the field of meteorological research and raise awareness of the issues and challenges of climate change. In dealing with climate change issues, the society of Oman has to focus on factors such as sustaining ecosystem, building eco house projects and developing water resources. Research on various indicators of climate change will provide scientific evidence for decision makers to help plan and formulate regulations and policies.

Acknowledgment

Conflict of interest

The authors declare that they have no conflict of interest.

References

[1] Al Charabi Y, Al-Yahyai S. Projection of future changes in rainfall and temperature patterns in Oman. J Earth Sci Clim Change. 2013;4(5):1–8.
[2] Al-Kalbani MS, John C, Martin F, et al. Recent trends in temperature and precipitation in Al Jabal Al Akhdar, Sultanate of Oman, and the implications for future climate change. Journal of Earth Science & Climatic Change. 2015;6(8):1.

[3] Buerkert A, Fernandez E, Tietjen B, Luedeling E. Revisiting climate change effects on winter chill in mountain oases of northern Oman. Climatic Change. 2020;162(3):1399–1417.

[4] Tonkaz T, Çetin M, Tülücü K. The impact of water resources development projects on water vapor pressure trends in a semi-arid region, Turkey. Climatic change. 2007;82(1-2):195–209.

[5] Shadmani M, Marofi S, Roknian M. Trend analysis in reference evapotranspiration using Mann-Kendall and Spearman's rho tests in arid regions of Iran. Water resources management. 2012;26(1):211–224.

[6] Golyandina N, Korobeynikov A, Zhigljavsky A. Singular spectrum analysis with R. Springer; 2018.

[7] Golyandina N, Nekrutkin V, Zhigljavsky AA. Analysis of time series structure: SSA and related techniques. CRC press; 2001.

[8] Golyandina N, Korobeynikov A. Basic singular spectrum analysis and forecasting with R. Computational Statistics & Data Analysis. 2014;71:934–954.

[9] Hassani H, Mahmoudvand R. Singular spectrum analysis: Using R. Springer; 2018.

[10] Pepelyshev A, Zhigljavsky A. SSA analysis and forecasting of records for Earth temperature and ice extents. Statistics and Its Interface. 2017;10(1):151–163.

[11] Harmouche J, Fourer D, Auger F, Borgnat P, Flandrin P. The sliding singular spectrum analysis: A data-driven nonstationary signal decomposition tool. IEEE Transactions on Signal Processing. 2017;66(1):251–263.

[12] Şen Z. Innovative trend analysis methodology. Journal of Hydrologic Engineering. 2012; 17(9):1042–1046.

[13] Kişi Ö, Guimaraes Santos CA, Marques da Silva R, Zounemat-Kermani M. Trend analysis of monthly streamflows using Sena's innovative trend method. Geofizika. 2018;35(1):53–68.

[14] Gedefaw M, Yan D, Wang H, Qin T, Girma A, Abiyu A, Batsuren D. Innovative trend analysis of annual and seasonal rainfall variability in Amhara regional state, Ethiopia. Atmosphere. 2018;9(9):326.

[15] Cui L, Wang L, Lai Z, Tian Q, Liu W, Li J. Innovative trend analysis of annual and seasonal air temperature and rainfall in the Yangtze river basin, China during 1960–2015. Journal of Atmospheric and Solar-Terrestrial Physics. 2017;164:48–59.

[16] Kondrashov D, Denton R, Shprits Y, Singer H. Reconstruction of gaps in the past history of solar wind parameters. Geophysical Research Letters. 2014;41(8):2702–2707.

[17] Korobeynikov A, Shlemov A, Usevich K, Golyandina N. Rssa: a collection of methods for singular spectrum analysis. R package version 013-1. 2015;Available from: http://CRAN.R-project.org/package=Rssa.

[18] Chong A, Lam KP, Xu W, Karaguzel OT, Mo Y. Imputation of missing values in building sensor data. ASHRAE and IBPSA-USA SimBuild. 2016;6:407–414.

[19] Yue S, Pilon P, Cavadias G. Power of the Mann–Kendall and Spearman's rho tests for detecting monotonic trends in hydrological series. Journal of hydrology. 2002;259(1-4):254–271.

[20] Şen Z. Innovative trend significance test and applications. Theoretical and applied climatology. 2017;127(3-4):939–947.

[21] Da Silva RM, Santos CA, Moreira M, Corte-Real J, Silva VC, Medeiros IC. Rainfall and river flow trends using Mann–Kendall and Sena's slope estimator statistical tests in the Cobres river basin. Natural Hazards. 2015;77(2):1205–1221.

[22] Silva RM, Silva JFCBC, Santos CAG, Silva AM, Brasil Neto RM. Spatial distribution and estimation of rainfall trends and erosivity in the Epitácio Pessoa reservoir catchment, Paraíba, Brazil. Natural Hazards. 2020;102:829–849.